PROCEEDINGS OF THE ROYAL SOCIETY B

Proc. R. Soc. B (2010) **277**, 2113–2120
doi:10.1098/rspb.2010.0075
Published online 17 March 2010

Morphological aspects of self-repair of lesions caused by internal growth stresses in stems of *Aristolochia macrophylla* and *Aristolochia ringens*

Sebastian Busch*, Robin Seidel, Olga Speck and Thomas Speck

Plant Biomechanics Group, Botanical Garden, Faculty of Biology, University of Freiburg, Schänzlestrasse 1, 79104 Freiburg, Germany

This study reveals in detail the mechanism of self-repair during secondary growth in the vines *Aristolochia macrophylla* and *Aristolochia ringens* based on morphological data. For a comprehensive understanding of the underlying mechanisms during the self-repair of lesions in the sclerenchymatous cylinder of the stem, which are caused by internal growth stresses, a classification of morphological changes in the cells involved in the repair process is required. In an early stage of self-repair, we observed morphological changes as a mere extension of the turgescent cortex cells surrounding the lesion, whereby the cell wall extends locally through visco-elastic/plastic deformation without observable cell wall synthesis. Later stages involve typical cell growth and cell division. Several successive phases of self-repair were investigated by light microscopy of stained samples and confocal laser-scanning microscopy in fluorescence mode. The results indicate that *A. macrophylla* and *A. ringens* respond to lesions caused by internal growth stresses with a sophisticated self-repair mechanism comprising several phases of different repair modes.

Keywords: *Aristolochia macrophylla*; *Aristolochia ringens*; self-healing; self-repair; vine; growth stress

1. INTRODUCTION

When thinking of self-repair in plants, wound healing and defence strategies are the first things that come into mind. For example, in vines, a variety of mechanisms of wound healing after external treatment have been shown, like callus formation and tissue regeneration (Wilson & Grange 1983; Dobbins & Fisher 1986; Fisher & Ewers 1989; Fisher 1991; Fordyce 2001). In addition to externally induced wounding, it was discovered that lesions (e.g. in the sclerenchymatous cylinder) also occur as a natural effect during ontogeny caused by internal growth stress owing to secondary growth (Haberlandt 1924; Rowe & Speck 2005; Speck *et al.* 2006*a*,*b*). Speck *et al.* (2004, 2006*b*) reported that various *Aristolochia* species show very efficient repair mechanisms in their stems. In young stems, *Aristolochia* species typically possess a closed cylinder of sclerenchymatous fibres in the stem periphery, responsible for high bending stiffness (Speck & Rowe 1994, 2003). As a consequence of secondary growth, phloem and especially xylem located within the sclerenchymatous cylinder significantly increase in size. The expansion of vascular cambial tissue causes stresses and strains in the adjacent outer and inner primary tissues. Whereas in the inner primary parenchymatous tissues mainly radial compressive stresses and strains occur, a combination of radial compressive and tangential tension stresses is found in the outer primary cortex cylinder. These stresses cause a compression of the pith, a collapse of large early wood vessels and a decrease in the radial width of the parenchymatous inner zone of the primary cortex owing to radial compressive strains. The sclerenchymatous outer cylinder finally ruptures radially owing to over-critical tangential stresses and strains that are in first-order approximation evenly distributed within the sclerenchymatous cylinder (Masselter & Speck 2008). These lesions finally lead to a segmentation of the sclerenchymatous cylinder that typically run through the middle lamellae of neighbouring sclerenchymatous cells. In detail, *Aristolochia macrophylla* reacts to lesions in its peripheral strengthening tissues with a repair mechanism sealing the lesions in the sclerenchymatous ring, thereby securing the functional integrity of the plant structure. Speck *et al.* (2004, 2006*a*,*b*) postulated that at least four discernable phases are involved in the fast repair mechanism of the sclerenchymatous cylinder in stems of *A. macrophylla*: elastic/visco-elastic deformation of the walls of the lesion-sealing parenchyma cells (phase I); plastic deformation of the cell walls (phase II); cell division in radial (phase IIIa) and tangential directions (phase IIIb); and finally the lignification of the (most peripheral) lesion-sealing cells (phase IV). Because it is not possible to distinguish between elastic/visco-elastic and plastic deformation of the lesion-sealing parenchymatous cell walls within an embedded cross-section, in this paper we use phase I + II as synonym for elastic/visco-elastic/plastic deformation of the wall. Speck *et al.* (2004, 2006*a*,*b*) proposed to use this fast repair mechanism as a biological concept generator for technical applications (e.g. a biomimetic fast repair coating for the membranes of pneumatic structures).

Vines of the genus *Aristolochia* seem especially suitable for a quantitative study of self-repair processes caused by internal stresses and strains owing to secondary growth as they show very efficient rapid repair mechanisms in their

* Author for correspondence (sebbusch@gmx.de).

Received 13 January 2010
Accepted 26 February 2010

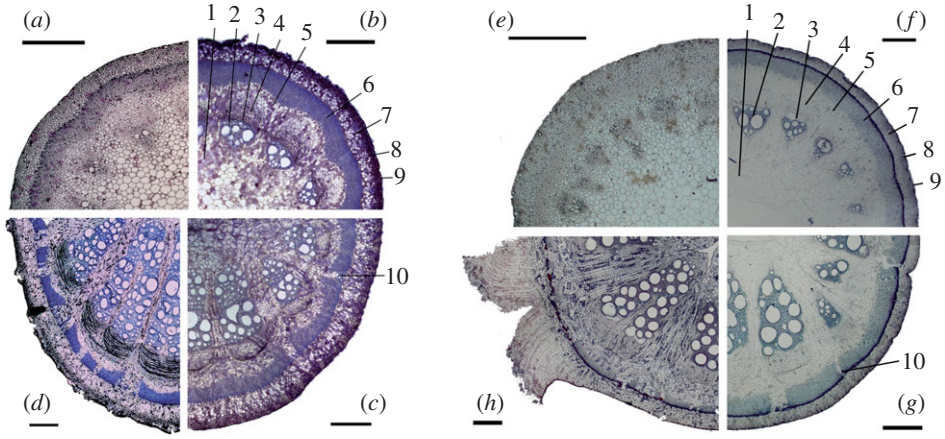

Figure 1. Transverse cross-sections of (*a–d*) *A. macrophylla* and (*e–h*) *A. ringens* showing different phases of ontogeny and the capability of self-repair. (*a*,*e*) The apical region of the axis is scarcely lignified. (*b*,*f*) In the approximately 1-year-old part of the same axis, the sclerenchymatous cylinder is uniformly lignified without lesions; the peripheral cell layers of the sclerenchymatous cylinder show thickened cell walls. 1, pith; 2, secondary xylem; 3, cambium; 4, secondary phloem; 5, inner parenchymatous cortex; 6, sclerenchymatous cylinder; 7, outer parenchymatous cortex; 8, collenchymatous cylinder; 9, epidermis. (*c*,*g*) The approximately 2-year-old part of the same axis shows several lesions (10) within the sclerenchymatous cylinder, caused by tangential tension owing to secondary growth. (*d*,*h*) Basal region of the axis. The sclerenchymatous cylinder is partly closed again by lignified parenchyma cells and has an increased perimeter. Scale bar, 500 μm.

stems. In this study, we present a detailed investigation of these mechanisms for the temperate North American species *A. macrophylla*, and compare the results with a species from tropical South America, *Aristolochia ringens*. Both species are woody vines, but belong to different subgenera. *Aristolochia ringens* belongs to the subgenus *Aristolochia*, whereas *A. macrophylla* belongs to *Siphisia* (Murata *et al.* 2001; Ohi-Toma *et al.* 2006). The comparison of the two *Aristolochia* species will contribute to a better understanding of the functional details of self-repair processes on a broader basis in the genus *Aristolochia*, and will allow answering of the question as to whether in the first phase of fissure repair the cell wall deforms as a whole or visco-elastic/plastic deformation occurs only locally.

2. MATERIAL AND METHODS

(a) *Plant material and specimen preparation*

Five stems of different size and age were taken from an individual plant of *A. macrophylla* Lam. cultivated outdoors in the Botanical Garden of the University of Freiburg, and one stem was taken from *A. ringens* Vahl. growing in the tropical greenhouse of the same botanical garden ($24 \pm 3^{\circ}$C; 80–90% relative humidity). Short segments of the stems were fixed in buffered glutaraldehyde, dehydrated in isopropanol and embedded in a methacrylate resin. Semi-thin sections (1–3 μm) were then prepared on a rotary microtome and stained with safranin/methylene blue according to Fink (1991, 1999) for bright-field microscopy. For confocal imaging, hand-cut sections of *A. macrophylla* were stored in 70 per cent ethanol, immersed in a saturated solution of acridine orange in methyl salicylate for several hours and washed with methyl salicylate before the images were recorded. To increase the optical penetration during scan acquisition, the samples were imaged in methyl salicylate (Gray *et al.* 1999).

(b) *Microscopy and data evaluation*

Cross-sections were imaged using bright-field illumination with an Olympus microscope equipped with a 100× oil immersion objective and an Olympus Dp71 camera. Series of three or four images of each cross-section were recorded with 1 μm increment to get the optimal focus on the cell wall thickness of the whole cell. Cell perimeter, cell area and cell wall thickness of the parenchyma cells involved in the self-repair mechanism were determined with the image analysis software ImageJ (v. 1.42k). Each measured cell and cell wall thickness was automatically numbered so that each measurement could later be correlated with its position. The cell wall area, which is the product of cell perimeter and cell wall thickness, and the circularity of the cell, which is a measure for the extent of deformation $\left(\text{circularity} = 4\pi \times (\text{area}/\text{perimeter}^2)\right)$, were calculated for each cell individually. All data were graphically represented using R (v. 2.8.1). We performed an analysis of variance (ANOVA) on ranks using Dunn's method with $p < 0.05$ or paired Student's *t*-test if appropriate with SigmaStat (v. 3.10, Systat Software Inc., Chicago, IL, USA).

Fluorescence imaging was accomplished using a Leica TCS-SP2 confocal laser-scanning microscope equipped with 20× objective. Serial images through *A. macrophylla* and *A. ringens* samples were recorded with a pixel resolution of 2048 × 2048 for 100 images in total, having a size depth of 37 μm (corresponding to a voxel size of 0.05 μm^3). For fluorescence excitation of acridine orange, $\lambda_1 = 458$ nm at 69 per cent relative power and $\lambda_2 = 476$ nm at 47 per cent relative power were chosen. Fluorescence emission of acridine orange was detected in a wavelength range from 500 to 650 nm. All images were further processed with ImageJ and are visualized as maximum-intensity z-projection plots.

3. RESULTS

(a) *Stem ontogeny*

The transverse cross-sections along single stems of *A. macrophylla* (figure 1*a–d*) and *A. ringens* (figure 1*e–h*) show different stages of ontogeny. In very young stem parts from the apical region of the axis (approx. 5 cm distance to the apex) the sclerenchymatous cylinder is visible but not lignified, and non-lignified protoxylem

cells are visible (figure 1*a*,*e*). In older stem parts of the same axis (approx. 1 m distance to the apex), the sclerenchymatous cylinder is lignified and entirely closed without lesions (figure 1*b*,*f*). The two peripheral cell layers of the sclerenchymatous cylinder of *A. ringens* show extremely thickened cell walls (wall thickness: 6.8 ± 1.2 μm), and the cell wall occupies about 96 ± 4 per cent of the cross-sectional cell area. In *A. macrophylla*, cell walls of the peripheral layers of the sclerenchymatous cylinder are less thickened (wall thickness: 3.5 ± 0.9 μm) and account for 52 ± 10 per cent of the cross-sectional cell area. Lignified cells are also visible in the xylem of the vascular segments where three to five vessels of large diameter exist. A more mature part of the same axis (approx. 2 m distance to the apex) shows several lesions within the sclerenchymatous cylinder and a compressed pith (figure 1*c*,*g*). The basal region of the stems, which are several years old (approx. 10 m distance to the apex), shows a widened sclerenchymatous cylinder with many fissures sealed by partly lignified cortex parenchyma cells (figure 1*d*,*h*). The xylem region now accounts for more than half of the cross-sectional area with bundles built of up to 20 large-diameter vessels. In both *A. macrophylla* and *A. ringens*, an even more compressed pith could be observed in these basal parts of the stems, owing to stresses and strains caused by secondary growth processes. The sclerenchymatous cylinder of *A. macrophylla* and *A. ringens* that is ruptured and split into segments as a consequence of vascular secondary growth in both species undergoes self-repair (figure 1*c*,*d*,*g*,*h*).

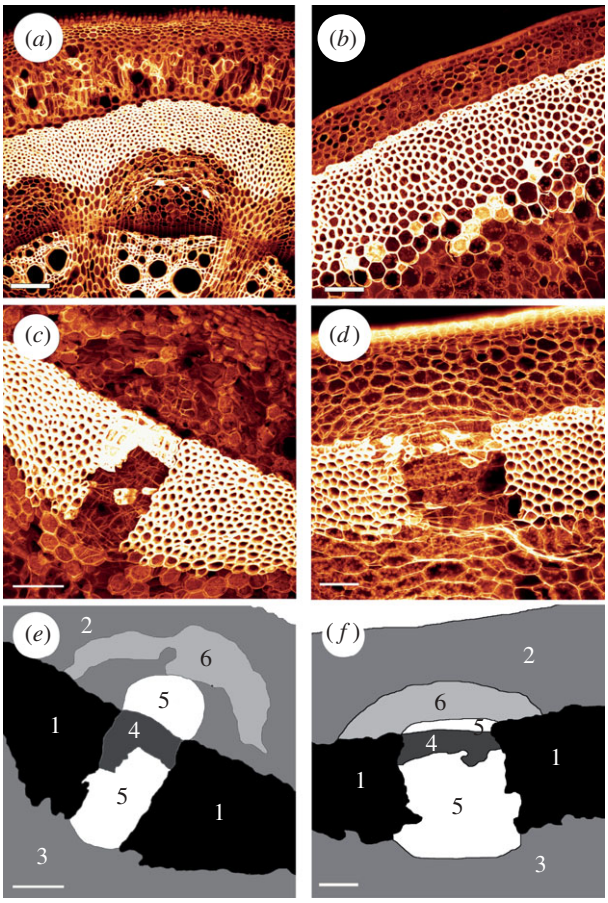

Figure 2. Cross-sections of (*a*,*c*,*e*) *A. macrophylla* and (*b*,*d*,*f*) *A. ringens* scanned with a confocal microscope. (*a*,*b*) The apical part of the plant without fissures in the sclerenchymatous cylinder. (*c*,*d*) An older part with repaired lesions of phase IV. (*e*,*f*) A sketch of the cell types of (*c*,*d*), with sclerenchyma (1), outer cortex parenchyma (2), inner cortex parenchyma (3), lignified peripheral repair cells (4), thin-walled parenchymatous repair cells (5) and tangentially strained cells of the outer primary parenchymatous cortex (6). Scale bar, 100 μm.

(b) *Morphological observations of the self-repair phases*

Confocal fluorescence microscopy allows detailed spatial information to be obtained on the self-repair in *A. macrophylla* and *A. ringens*. For comparison, both *Aristolochia* taxa were monitored in young stages showing no lesions and no repair processes (figure 2*a*,*b*). In these young stem segments, the parenchymatous cells of the outer cortex are uniformly distributed and show no deformation.

Figure 2*c*, depicting a stem segment of *A. macrophylla* in repair phase IV, shows the cell types and their respective deformations in the vicinity of repaired lesion. In addition to the cells directly involved in the repair process (cell types 4 and 5 in figure 2*e*), cells of the outer parenchymatous cortex located distally to the lesion show distinct deformations (cell type 6 in figure 2*e*). These cells, which are found in concentric bands in a crescent-shaped region peripheral to the lesion, are tangentially strained and show undulated radial cell walls.

In *A. ringens*, a similar pattern in repaired lesions of phase IV and a similar deformation of the cortex parenchyma cells are observed (figure 2*d*). Tangentially strained cortex cells, arranged in a crescent-shaped region are visible (cell type 6 in figure 2*f*) as in *A. macrophylla*, yet not as pronounced, and undulated cell walls are scarcely present in *A. ringens*. All other cell types can be attributed according to the classification given in figure 2*f*.

Figure 3 shows exemplarily the different phases of self-repair in both species. Figure 3*a*,*f* shows the initial phases (phase I + II) of self-repair. As soon as (even tiny) lesions in the blue-stained sclerenchymatous cylinder occur, parenchyma cells from the surrounding outer cortex tissue swell into this lesion and immediately start to seal it. In older ontogenetic stages, when the lesion has increased owing to ongoing secondary vascular growth, the repair cells start to divide tangentially (figure 3*b*,*g*) and are tightly attached to the surface of the lesion (phase IIIa). In phase IIIb, when the size of the fissure has further increased and the fissure runs through the entire sclerenchymatous ring, an increased radial and tangential cell division can be observed (figure 3*c*,*h*), ensuring a tight sealing of the lesion. In the fourth repair phase, the cell walls of the most peripheral sealing cells start to thicken and lignify (figure 3*d*, *i*), and thereby, in addition to sealing the lesion, also partly restore the mechanical function of the sclerenchymatous cylinder. This process continues with the increasing tangential width of the lesions (figure 3*e*, *j*) until finally in old stems the newly built repair cells remain unlignified and the sclerenchymatous cylinder is fractured in isolated segments. The peripheral collenchymatous cylinder remains unaffected during this repair process.

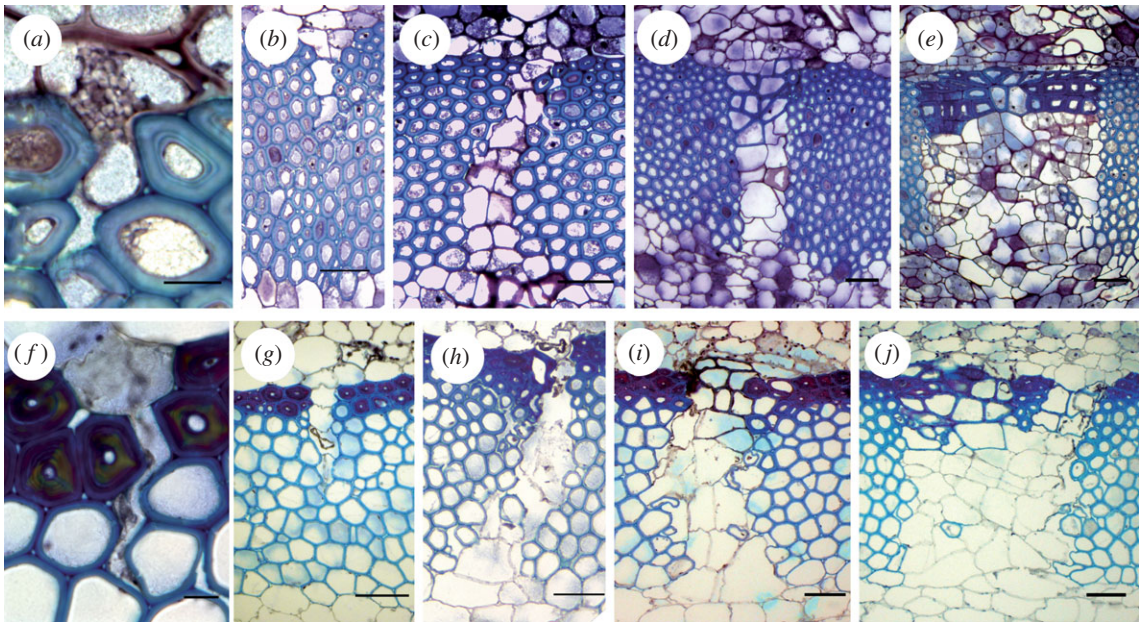

Figure 3. Self-repair phases in (*a–e*) *A. macrophylla* and (*f–j*) *A. ringens*. (*a*,*f*) In the initial phases (I + II) of self-repair, a lesion in the blue-stained sclerenchymatous cylinder is sealed with a plasticized parenchyma cell. (*b*,*g*) In the subsequent phase (III) of self-repair, a bigger lesion is filled with thin-walled, irregularly shaped cells. (*c*,*h*) Cell division first occurs in the radial direction, and later in increasingly broad lesions in the tangential direction. (*d*,*e*,*i*,*j*) The cell walls of repairing parenchyma cells lying in the most peripheral region of the lesion are thickened and lignified, thereby—at least partly—restoring the stability of the sclerenchyma cylinder (phase IV of self-repair). Scale bars, (*a*,*f*) 10 μm and (*b–e*,*g–j*) 50 μm.

(c) *Quantitative investigations of the self-repair phases*

To quantify the self-repair mechanisms in *A. macrophylla* and *A. ringens* in detail, the dimensions of the cells and cell walls in cross-sections representing different repair phases were measured with ImageJ. In all stems, cortex parenchyma cells were found, which could be attributed to repair phase I + II. It can be seen that the repair cell expands into a newly formed lesion within the sclerenchymatous cylinder (stained blue) and fills, or rather seals, this lesion (figure 3*a*,*f*). As shown in figure 4*a*, the repair cells of phase I + II were subdivided for further analysis into a cortex-sided part and a sclerenchyma-sided part filling the lesion. In total, four parameters were evaluated in each cell: cross-sectional area, perimeter, wall thickness and cross-sectional area of the wall.

The cross-sectional area of *A. macrophylla* repair cells in phase I + II is almost identical to the cross-sectional area of 'normal' cortex parenchyma cells, whereas in *A. ringens* the cell area for phase I + II repair cells is higher, but not significantly (table 1). In both species, the mean of the cross-sectional area of phase III and IV repair cells is higher than in phase I + II repair cells, but not significantly. The same holds for the cross-sectional area of phase III and IV repair cells compared with normal parenchyma cells in *A. macrophylla*, whereas in *A. ringens*, phase III and IV repair cells show a significantly higher cross-sectional area than normal parenchyma cells (Dunn's test, $p < 0.05$; table 1).

The perimeter of the repair cells (phase I + II) in both species is not significantly different from normal cortex parenchyma cells (table 1). In *A. macrophylla* also, the perimeter of phases III and IV does not differ significantly from normal parenchyma cells, whereas for *A. ringens*, the cell perimeter for cells of the repair phases III and IV is significantly higher than in normal parenchyma cells (Dunn's test, $p < 0.05$). The circularity of the repair cell of phases I + II and III is significantly lower than the circularity of the normal cortex parenchyma cells in both species (figure 5*c*,*d* and table 1). This proves that the cells in the first repair phases are significantly more irregularly shaped than normal cortex parenchyma cells. In both species, the circularity of phase IV repair cells differs not significantly from normal cortex parenchyma cells.

Considering the cell wall thickness in both *Aristolochia* species in phase I + II, the part that fills the lesion within the sclerenchymatous cylinder possesses a significantly thinner cell wall than the part of the cell in the cortex (paired *t*-test, $p = 0.016$ for *A. macrophylla*, $n = 7$; $p < 0.0001$ for *A. ringens*, $n = 9$; figure 4*b*,*c* and table 1). The cell wall of the sclerenchyma side of the repair cells is also thinner than the wall of normal cells of the outer parenchymatous cortex in both species, whereas the cortex side shows no significant differences (figure 4*b*,*c*). In phase III, the wall thickness of the repair cells further decreases, while in phase IV the cell wall thickness increases by a factor of approximately 8 (table 1) and the cell walls become distinctly lignified (cf. figure 3*e*,*j*). The cell walls of the normal cortex parenchyma cells and the repair cells in phases I–III of *A. ringens* are significantly thinner than the cell walls of the respective cells of *A. macrophylla*, whereas the cell walls of the peripheral sclerenchyma cells of *A. ringens* are significantly thicker compared with *A. macrophylla* (Dunn's test, $p < 0.05$).

In both species, the cell wall area (i.e. the area of the cell wall within a cross section), which is calculated by the product of perimeter and mean cell wall thickness, does not differ significantly between repair cells of phases I + II and III and the normal cells of the outer

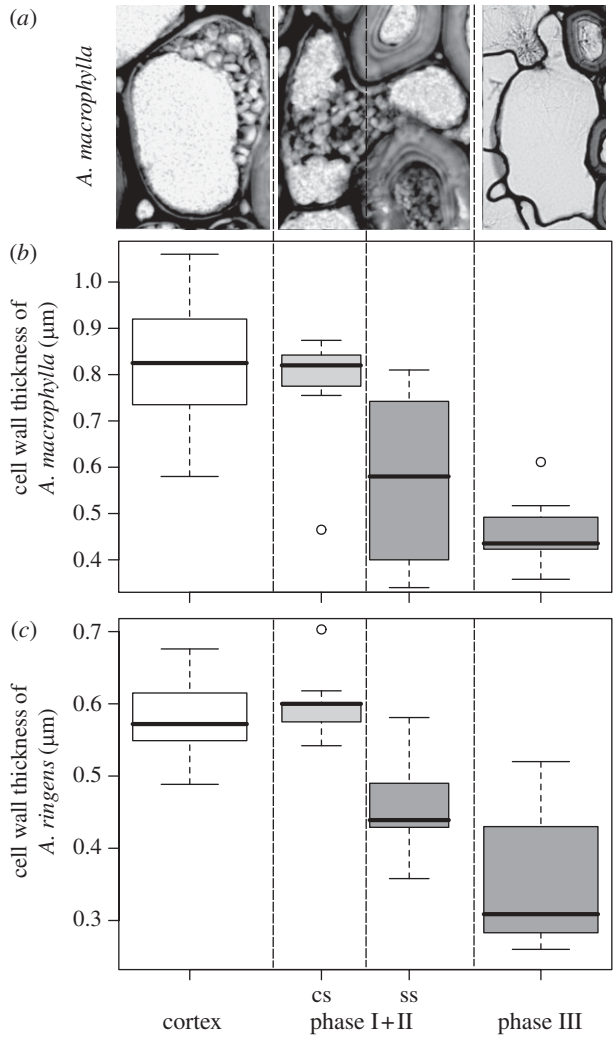

Figure 4. (*a*) Exemplary images of *A. macrophylla* cells in different repair phases for quantitative measurements. (*b*,*c*) Box plots of the cell wall thickness of the repair cells of (*b*) *A. macrophylla* and (*c*) *A. ringens*. Cells of the normal outer cortex parenchyma are compared with repair cells of phases I + II and III. Phase I + II cells are subdivided into a cortex-sided (cs) part and the sclerenchyma-sided (ss) part filling the lesion. There is a significant difference between the cs part and the ss part of phase I + II repair cells and between the normal cortex parenchyma cells and phase III repair cells in both species. In phase IV, the cell wall thickness increases significantly to approximately 3 μm thickness (table 1).

parenchymatous cortex (figure 5 and table 1). Yet in phase IV the cell wall area increases significantly, correlating with the observed increase in cell wall thickness (Dunn's test, $p < 0.05$).

4. DISCUSSION AND CONCLUSION

In this study, we analysed quantitatively the self-repair processes in the outer sclerenchymatous cylinder of *A. macrophylla* and *A. ringens*. According to our findings, the observed self-repair is a consequence of ontogeny-related lesions caused by internal growth stresses and strains owing to secondary vascular growth (Masselter & Speck 2008). In addition to radial and tangential stresses and strains in the primary cortex tissues peripheral to the secondary phloem, these stresses also cause compression of the parenchymatous pith in older stem parts of *A. ringens*, which are similar to the ones described for stems of *A. macrophylla* (Masselter & Speck 2008). The increasing secondary growth of vascular cambial tissues causes mainly radial stresses and strains in the inner primary parenchymatous cortex of both *Aristolochia* species, resulting in a tangential flattening of these cells. In the sclerenchymatous cylinder, radial and tangential stresses and strains occur that finally lead to a rupturing of this cylinder if the critical values are reached (Masselter & Speck 2008). These lesions are sealed and repaired by repair cells originating from the outer primary parenchymatous cortex. The increase in perimeter of the sclerenchymatous cylinder owing to increasing tangential widening of the lesion during increasing secondary vascular growth also affects more peripheral regions of the outer parenchymatous cortex. The increase in perimeter is mirrored by crescent-shaped regions of radially compressed and tangentially strained cells in the outer parenchymatous cortex located distally to each of the repaired lesions. The radial compression in the cells of the crescent-shaped regions leads to an undulation of the radial cell walls being more pronounced in *A. macrophylla* than in *A. ringens*. In regions of the outer cortex not adjacent to the fissures, no radial compression and no tangential straining of the parenchymatous cortex cells are visible. Together with the ongoing repair of the lesions, this allows the stems to cope with the increase in size of the inner vascular tissues during the first phases of secondary growth. The lesions in the sclerenchymatous cylinder are usually found not peripheral to the vascular bundles themselves but in the region of the wood rays between two vascular bundles. This is due to the fact that the secondary growth of the vascular bundles leads to high tangential strains, especially in the segments of the sclerenchymatous ring that are located above the wood rays between two bundles.

The peripheral collenchymatous cylinder is not visibly affected by these internal growth stresses and strains, and the epidermis is still complete in these growth phases and can protect the stem from possible water loss and against infections owing to surface cracks. In older ontogenetic stages, a distinct formation of periderm takes place, which typically starts peripheral to the repaired lesions. This periderm that can cope with further increase in stem diameter represents the outer 'protection tissue' of older stems in both *Aristolochia* species.

If an internal lesion caused by the rupture of the sclerenchymatous cylinder occurs, the adjacent parenchyma cells will immediately deform, owing to relaxation processes caused by the changes in the stress–strain field at the contact region between fissure and parenchymatous tissues, and swell into the lesion (phase I). This fast process is a passive physical reaction of the repair cells causing an elastic/visco-elastic deformation of these cells. In the next phase (II), first physiological reactions in the repair cells occur, leading to a plasticization of the cell walls (cell wall loosening). As soon as cell wall loosening starts, plastic deformation increasingly dominates the process. From our data, we cannot discern between an elastic/visco-elastic or plastic deformation as the embedding process fixates the actual state. However, from theoretical considerations (see above) as well as from first physiological and biochemical results (not

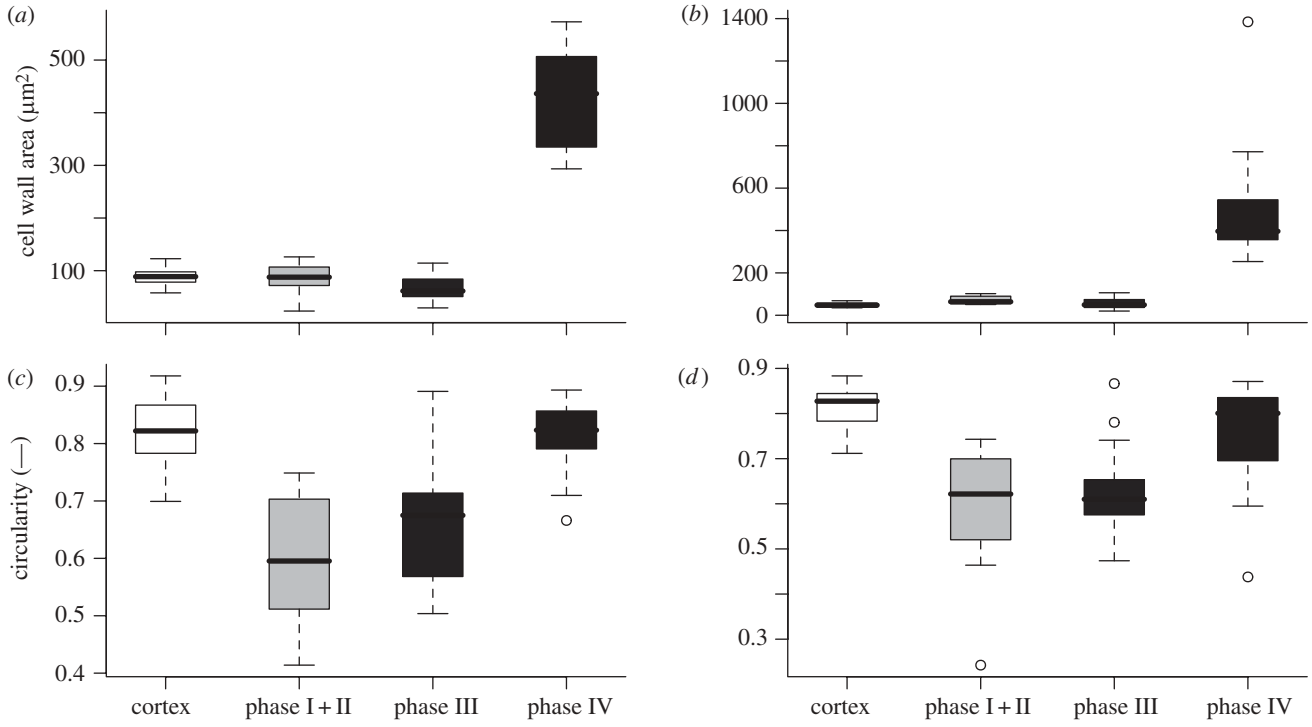

Figure 5. Box plots of (*a*,*b*) cell wall area and (*c*,*d*) circularity of (*a*,*c*) *A. macrophylla* and (*b*,*d*) *A. ringens*. There is no significant difference in cell wall area between normal parenchyma cells and repair cells of phases I–III in either species, whereas in phase IV, the cell wall area increases significantly. The circularity of repair cells of phases I + II and III is significantly smaller than the circularity of normal cortex cells and repair cells of phase IV in both species.

Table 1. Morphometric data of repairing cells of the four repair phases of *A. macrophylla* and *A. ringens* compared with normal cells of the outer cortex parenchyma and peripheral sclerenchyma cells of the sclerenchymatous cylinder (mean ± s.d.). The cell wall thickness of phase I + II is subdivided into the cortex-sided (cs) part of the cell and the part that fills the lesion within the sclerenchyma cylinder (ss). The cs part is significantly thicker than the ss part in repair phase I + II in both *A. macrophylla* and *A. ringens*. Different letters (a, b, c, d) indicate significant differences between cell types and different repair phases within one species (ANOVA on ranks, Dunn's Method, $p < 0.05$).

cell type		cell area (μm^2)	cell perimeter (μm)	cell circularity (—)	cell wall thickness (μm)	cell wall area (μm^2)	*n*
A. macrophylla							
cortex		746 ± 180 a	106 ± 13 a	0.82 ± 0.06 a	0.83 ± 0.12 a	88 ± 16 a	24
	cs				0.77 ± 0.14*		
phase I + II		626 ± 327 ab	112 ± 34 a	0.60 ± 0.13 b	0.73 ± 0.15 a	85 ± 34 a	7
	ss				0.57 ± 0.20*		
phase III		1146 ± 723 a	141 ± 42 a	0.67 ± 0.11 bc	0.45 ± 0.06 b	64 ± 23 a	14
phase IV		975 ± 531 a	119 ± 31 a	0.81 ± 0.07 ac	3.67 ± 0.77 c	424 ± 86 b	14
peripheral sclerenchyma		217 ± 81 b	53 ± 11 b	0.91 ± 0.03 d	3.53 ± 0.93 c	194 ± 74 b	14
A. ringens							
cortex		472 ± 173 a	84 ± 16 ac	0.81 ± 0.05 ab	0.58 ± 0.06 a	49 ± 11 a	14
	cs				0.60 ± 0.05***		
phase I + II		726 ± 176 ab	130 ± 38 ab	0.59 ± 0.16 c	0.54 ± 0.06 ab	71 ± 20 a	9
	ss				0.45 ± 0.06***		
phase III		1337 ± 873 b	154 ± 52 b	0.63 ± 0.10 c	0.35 ± 0.08 b	55 ± 27 a	14
phase IV		1278 ± 434 b	146 ± 33 b	0.75 ± 0.12 a	3.38 ± 1.49 c	497 ± 288 b	15
peripheral sclerenchyma		215 ± 81 c	54 ± 10 c	0.90 ± 0.03 b	6.76 ± 1.24 c	376 ± 134 b	14

*Paired *t*-test, p=0.016.
***Paired *t*-test, $p = 0.00007$.

detailed here), we have good evidence that there exist two initial phases of first (mainly) elastic/visco-elastic deformation and then (mainly) plastic deformation.

Our results support the hypothesis that at least four self-repair phases in both *Aristolochia* species can be discerned. In a first step (phases I and II), an internal lesion caused by the rupture of the sclerenchymatous cylinder is sealed mainly owing to an elastic/visco-elastic or plastic deformation of turgescent, adjacent parenchyma cells of the outer primary cortex that swell into the

lesion. In the following step (phase III), the repairing parenchyma cells undergo cell division, first in radial and then in tangential direction, and tightly seal the lesion that increases in width.

Considering the investigated parameters (cell wall thickness, cell area, cell perimeter, cell wall area and circularity) in detail, we found that for repair cells of phase I + II, the cell wall thickness of the lesion-sealing part is significantly thinner compared with the part of the cell wall in the cortex region in both *Aristolochia* species. The latter equals the wall thickness of normal parenchymatous cells. This supports the hypothesis of an initial rapid self-repair phase characterized by local (visco-)elastic/plastic deformation of (parts of) the repairing cells from the outer primary parenchymatous cortex that swell into the lesions and seal them. A further finding is that in both *A. macrophylla* and *A. ringens*, the cell wall area does not differ significantly in repairing cells of phase I + II compared with normal reference cells in the outer parenchymatous cortex. Therefore, it can be assumed that in the initial self-repair phase I + II, a synthesis of new cell wall material does not take place. This supports our hypothesis of the (mainly) physico-chemical character of the initial phases (I + II) of the rapid self-repair where a deformation of the cell wall owing to external mechanical stresses and/or a loosening of the cell wall by biochemical reagents occurs.

In phase IV of the repair, the cell wall thickness as well as the cell wall area of the peripheral repair cell increases drastically in both species. This is accompanied by a lignification of the cell walls. This allows—in addition to sealing the increasingly wide lesions—at least partly to restore the mechanical function of the sclerenchymatous cylinder.

In both studied *Aristolochia* species, the repair processes are very similar in the sequence of the different repair phases and to the overall patterns found in the different phases. However, it is noticeable that in self-repair phase IV *A. ringens*—compared with *A. macrophylla*—forms a thicker-walled and a more lignified outer layer of repair cells in the repaired regions connecting sclerenchymatous segments of the sclerenchymatous cylinder. This is consistent with the finding that in the intact sclerenchymatous ring, the peripheral sclerenchyma cells (typically two or three cell rows) have nearly twice as thick cell walls in *A. ringens* than in *A. macrophylla*. It can be hypothesized that this peripheral sclerenchyma cell layer is of higher importance for mechanical stability in *A. ringens* than in *A. macrophylla* in stems with intact as well as in stems with repaired sclerenchymatous cylinder.

The circularity, a measure for the amount of cell shape irregularity, shows a significant decrease within the first three repair phases of *A. macrophylla* and *A. ringens*. This is consistent with the preliminary results of Speck *et al.* (2004) and shows that the shape of the repair cells is well adapted to the irregular shape of the lesions, and therefore can seal the lesions very effectively. In conclusion, our data support the hypothesis of a fast initial deformation of turgescent parenchyma cells for lesion repair without new cell wall synthesis to a large extent.

The tight sealing of the irregularly shaped fissures by the repairing cells indicates that a plasticization of their cell walls takes place during the repair process. Several mechanisms were proposed to be involved in cell wall plasticization during cell growth: (i) the production of reactive oxygen species (ROS), such as hydroxyl radicals, as reported by Liszkay *et al.* (2004) and Schopfer *et al.* (2002), causing a cleavage of the cellulose microfibrils; or (ii) proteins such as expansins, xyloglucan endotransglucosylase/hydrolases or endo-(1,4)-β-D-glucanases causing the cell walls to expand (Cosgrove 1999, 2005). Independent of which theory finally holds true, our study shows that cell wall loosening also plays an important role in self-repair processes. Cellular deformations during repair processes may represent an interesting model to evaluate current hypotheses of cell wall loosening. Takeda *et al.* (2008) showed that, for *Arabidopsis* root hairs, a local positive feedback mechanism involving the proteins RHD2, ROS and Ca^{2+} can determine cell shape. The finding that repair cells in *Aristolochia* deform locally allows us to hypothesize that there may be a similar active mechanism causing cell deformation during the first phase of self-repair.

In further experiments, micro-mechanical tension measurements would be necessary to determine whether the repair cells show an elastic/visco-elastic or plastic deformation in repair phase I + II. Yet, to date, the small size and inaccessibility of the cells in the investigated *Aristolochia* species do not allow a mechanical analysis on a single-cell level within the intact tissue arrangement.

This work was supported by the scholarship programme (Bionics) of the German Federal Environmental Foundation DBU. We gratefully acknowledge the preparation of plant cross-sections by the group of Siegfried Fink, University of Freiburg and the support of the staff of the Botanical Garden Freiburg during plant cultivation.

REFERENCES

Cosgrove, D. J. 1999 Enzymes and other agents that enhance cell wall extensibility. *Annu. Rev. Plant Physiol. Plant Mol. Biol.* **50**, 391–417. (doi:10.1146/annurev.arplant.50.1.391)

Cosgrove, D. J. 2005 Growth of the plant cell wall. *Nat. Rev. Mol. Cell Biol.* **6**, 851–861. (doi:10.1038/nrm1746)

Dobbins, D. R. & Fisher, J. B. 1986 Wound responses in girdled stems of lianas. *Bot. Gaz.* **147**, 278–289. (doi:10.1086/337595)

Fink, S. 1991 Comparative microscopical studies on the patterns of calcium oxalate distribution in various conifer species. *Bot. Acta* **104**, 306–315.

Fink, S. 1999 Pathological and regenerative plant anatomy. In *Encycl. plant anatomy XIV*, vol. XII, p.1095. Berlin, Stuttgart: Gebrüder Borntraeger.

Fisher, J. B. 1991 Structural responses to stem injury in vines. In *The biology of vines* (eds F. E. Putz & H. A. Mooney), pp. 99–124. Cambridge, UK: Cambridge University Press.

Fisher, J. B. & Ewers, F. W. 1989 Wound healing in stems of lianas after twisting and girdling injuries. *Bot. Gaz.* **150**, 251–265. (doi:10.1086/337770)

Fordyce, J. A. 2001 The lethal plant defense paradox remains: inducible host-plant aristolochic acids and the growth and defense of the pipevine swallowtail. *Entomol. Exp. Appl.* **100**, 339–346. (doi:10.1023/A:1019249306992)

Gray, J. D., Kolesik, P., Høj, P. B. & Coombe, B. G. 1999 Technical advance: confocal measurement of the three-dimensional size and shape of plant parenchyma cells in a developing fruit tissue. *Plant J.* **19**, 229–236. (doi:10.1046/j.1365-313X.1999.00512.x)

Haberlandt, G. 1924 *Physiologische Pflanzenanatomie*, 6th edn. Leipzig, Germany: Engelmann.

Liszkay, A., van der Zalm, E. & Schopfer, P. 2004 Production of reactive oxygen intermediates ($O^{2\bullet-}$, H_2O_2, and $^{\bullet}OH$) by maize roots and their role in wall loosening and elongation growth. *Plant Physiol.* **136**, 3114–3123. (doi:10.1104/pp.104.044784)

Masselter, T. & Speck, T. 2008 Quantitative and qualitative changes in primary and secondary stem organization of *Aristolochia macrophylla* during ontogeny: functional growth analysis and experiments. *J. Exp. Bot.* **59**, 2955–2967. (doi:10.1093/jxb/ern151)

Murata, J., Ohi, T., Wu, S., Darnaedi, D., Sugawara, T., Nakanishi, T. & Murata, H. 2001 Molecular phylogeny of *Aristolochia* (Aristolochiaceae) inferred from matK sequences. *Acta Phytotax. Geobot.* **52**, 75–83.

Ohi-Toma, T., Sugawara, T., Murata, H., Wanke, S., Neinhuis, C. & Murata, J. 2006 Molecular phylogeny of *Aristolochia sensu lato* (Aristolochiaceae) based on sequences of *rbcL*, *matK*, and *phyA* genes, with special reference to differentiation of chromosome numbers. *Syst. Bot.* **31**, 481–492.

Rowe, N. P. & Speck, T. 2005 Plant growth forms: an ecological and evolutionary perspective. *New Phytol.* **166**, 61–72. (doi:10.1111/j.1469-8137.2004.01309.x)

Schopfer, P., Liszkay, A., Bechtold, M., Frahry, G. & Wagner, A. 2002 Evidence that hydroxyl radicals mediate auxin-induced extension growth. *Planta* **214**, 821–828. (doi:10.1007/s00425-001-0699-8)

Speck, T. & Rowe, N. P. 1994 Bending stability of plant stems: ontogenetical, ecological, and phylogenetical aspects. *Biomimetics* **2**, 109–128.

Speck, T. & Rowe, N. P. 2003 Modelling primary and secondary growth processes in plants: a summary of the methodology and new data from an early lignophyte. *Phil. Trans. R. Soc. Lond. B* **358**, 1473–1485. (doi:10.1098/rstb.2003.1347)

Speck, T., Masselter, T., Prüm, B., Speck, O., Luchsinger, R. & Fink, S. 2004 Plants as concept generators for biomimetic lightweight structures with variable stiffness and self-repair mechanisms. *J. Bionics Eng.* **1**, 199–205.

Speck, O., Luchsinger, R., Busch, S., Rüggeberg, M. & Speck, T. 2006*a* Self-repairing membranes for pneumatic structures: transferring nature's solutions into technical applications. In *Proc. of the 5th Int. Plant Biomechanics Conf.*, vol. 1 (ed. L. Salmen), pp. 115–120. Stockholm, Sweden: STFI Packforsk AB.

Speck, T., Luchsinger, R., Busch, S., Rüggeberg, M. & Speck, O. 2006*b* Self-healing processes in nature and engineering: self-repairing biomimetic membranes for pneumatic structures. In *Design and nature III* (ed. C. A. Brebbia), pp. 105–114. Southampton, UK: WIT Press.

Takeda, S., Gapper, C., Kaya, H., Bell, E., Kuchitsu, K. & Dolan, L. 2008 Local positive feedback regulation determines cell shape in root hair cells. *Science* **319**, 1241–1244. (doi:10.1126/science.1152505)

Wilson, J. & Grange, R. 1983 Regeneration of sclerenchyma in wounded dicotyledon stems. *Ann. Bot.* **52**, 295–303.